

This is the author-created version of the following work:

**Silva, Catarina N.S., Murphy, Nicholas P., Bell, James J., Green, Bridget S.,  
Duhamel, Guy, Cockcroft, Andrew C., Hernández, Cristián E., and Strugnell,  
Jan M. (2020) *Global drivers of recent diversification in a marine species complex.*  
*Molecular Ecology*, .**

Access to this file is available from:

<https://researchonline.jcu.edu.au/65778/>

© 2020 John Wiley & Sons Ltd. The Author Accepted Manuscript is available from ResearchOnline@JCU from 21 December 2021. This article may be used for non-commercial purposes in accordance with Wiley Terms and Conditions for Use of Self-Archived Versions.

Please refer to the original source for the final version of this work:

<http://doi.org/10.1111/mec.15780>

# Global drivers of recent diversification in a marine species complex

Catarina N.S. Silva<sup>1,\*</sup>, Nicholas P. Murphy<sup>2</sup>, James J. Bell<sup>3</sup>, Bridget S. Green<sup>4</sup>, Guy Duhamel<sup>5</sup>, Andrew C. Cockcroft<sup>6</sup>, Cristián E. Hernández<sup>7,8</sup>, Jan M. Strugnell<sup>1, 2</sup>

<sup>1</sup> Centre for Sustainable Tropical Fisheries and Aquaculture and College of Science and Engineering, James Cook University, Townsville, Qld 4810, Australia

<sup>2</sup> Department of Ecology, Environment & Evolution, La Trobe University, Melbourne, Vic 3086, Australia

<sup>3</sup> School of Biological Sciences, Victoria University of Wellington, Wellington, 6140, New Zealand

<sup>4</sup> Institute for Marine and Antarctic Studies, University of Tasmania, Hobart, TAS 7001, Australia

<sup>5</sup> Département Adaptations du Vivant, BOREA, MNHN, Paris, 75005, France

<sup>6</sup> Department of Agriculture, Forestry and Fisheries, Cape Town, 8012, South Africa

<sup>7</sup> Departamento de Zoología, Facultad de Ciencias Naturales y Oceanográficas, Universidad de Concepción, Casilla 160C, Concepción, Chile

<sup>8</sup> Universidad Católica de Santa María, Arequipa, Perú

\*Corresponding author: catari.bio@gmail.com, +61 0434 685 673

**Running title:** Global drivers of diversification in lobsters

**Keywords:** demographic inference, environmental association, genomics, *Jasus* spp., lobsters, speciation-with-gene-flow

## Abstract

Investigating historical gene flow in species complexes can indicate how environmental and reproductive barriers shape genome divergence during speciation. The processes influencing species diversification under environmental change remain one of the central focal points of evolutionary biology, particularly for marine organisms with high dispersal potential. We investigated genome-wide divergence, introgression patterns and inferred demographic history between species pairs of all six extant rock lobster species (*Jasus* spp.), which have a long larval duration of up to two years and have populated continental shelf and seamount habitats around the globe at approximately 40°S. Genetic differentiation patterns reflected geographic isolation and the environment (i.e. habitat structure). Eastern Pacific species (*J. caveorum* and *J. frontalis*) were geographically more distant and genetically more differentiated from the remaining four species. Species associated with continental shelf habitats shared a common ancestry, but are geographically distant from one another. Similarly, species associated with island/seamount habitats in the Atlantic and Indian Oceans shared a common ancestry, but are also geographically distant. Benthic temperature was the environmental variable that explained most of the genetic differentiation ( $F_{ST}$ ), while controlling for the effects of geographic distance. Eastern Pacific species retained a signal of strict isolation following ancient migration, whereas species pairs from Australia and Africa, and seamounts in the Indian and Atlantic oceans, included events of introgression after secondary contact. Our results reveal important effects of habitat and demographic processes on the recent divergence of species within the genus *Jasus*, providing one of the first empirical studies of genome-wide drivers of diversification that incorporates all extant species in a marine genus with long pelagic larval duration.

## Introduction

The discrete categorization of speciation modes as sympatric, allopatric or parapatric is now considered to be overly simplistic (Butlin *et al.* 2008). Several events (or modes of speciation) can influence the biogeographic states of populations at different time periods during divergence, and as a result, the speciation process is now generally considered to be gradual and reticulated (Smadja & Butlin 2011; Feder *et*

53 *al.* 2012). However, the processes responsible for influencing species diversification are still poorly understood  
54 and remain one of the central focal points of ecology and evolutionary biology (Arendt *et al.* 2016).

55         Reconstructing the diversification history of marine species complexes can be challenging (e.g. Palero  
56 *et al.* 2009; Momigliano *et al.* 2017) as many have weak genetic differentiation (Ovenden 2013). For marine  
57 species, it is often difficult to determine whether weak genetic differentiation is actually present (e.g. as a  
58 result of the potential for long distance dispersal) or masked by large population sizes (Lowe & Allendorf 2010).  
59 In addition, marine species with long distance dispersal can quickly fill available niches, leaving fewer  
60 opportunities for *in situ* cladogenesis (Pinheiro *et al.* 2017). As a result, only a few studies have estimated  
61 demographic history from genomic data in marine species (e.g. Crow *et al.* 2010; Le Moan *et al.* 2016;  
62 Momigliano *et al.* 2017; Souissi *et al.* 2018; Titus *et al.* 2019).

63         Changes in the distribution of marine species resulting from historical climatic variation have been an  
64 important driver of diversification across taxa (Davis *et al.* 2016). Climatic fluctuations during the late  
65 Pleistocene, in particular, resulted in periods of isolation intercalated by contact and gene flow between  
66 lineages (Hewitt 2000). These glaciation events dramatically transformed available habitat causing major shifts  
67 in species distribution ranges and shaped the genetic structure of many marine species worldwide. For  
68 example, Pleistocene glaciations shaped contemporary genetic structure of the abalone *Haliotis asinina* in the  
69 Indo-Pacific (Benardine Jeffrey *et al.* 2007), the American lobster, *Homarus americanus*, along the  
70 northeastern coast of North America (Kenchington *et al.* 2009), and the octopod *Pareledone turqueti* in the  
71 Southern Ocean (Strugnell *et al.* 2012). Pleistocene glaciations were also responsible for the divergence of  
72 species complexes, such as the Damselfishes *Pomacentrus coelestis* (Sorenson *et al.* 2014) and the capelin  
73 *Mallotus villosus* (Dodson *et al.* 2007; Cayuela *et al.* 2020). Sequential glacial and interglacial periods have then  
74 further shaped the divergence history of species as a result of periods of isolation intercalated by gene flow  
75 (Weigelt *et al.* 2016). A better understanding of the species-specific historical context of divergence is  
76 therefore needed to estimate the actual timing and role of gene flow during speciation. Understanding how  
77 historical climatic fluctuations shaped species divergence provides clues on how species might respond to

future environmental changes, which is vital for effective conservation and management plans (Olivieri *et al.* 2016).

Advances in next-generation sequencing (NGS) now provide the opportunity to investigate genome-wide patterns of differentiation along the speciation continuum, allowing the better detection of changes as two lineages diverge from one another on the path to reproductive isolation (Feder *et al.* 2012). In particular, these methods provide effective tools for species with no reference genomes (Catchen *et al.* 2017), which is the case for many marine species including rock lobsters (Silva *et al.* 2019). This technology has also allowed the integration of genomic and environmental data which can be used for testing the hypothesis that selection is more efficient than drift in opposing the homogenizing effects of migration (Manel & Holderegger 2013). In addition, this approach can also detect candidate markers underlying adaptation to local environments for species with moderate to long distance dispersal potential (e.g. Benestan *et al.* 2016; Sandoval-Castillo *et al.* 2018). This robust approach is particularly useful in the marine environment where isolation and speciation is increasingly found to be associated with selection/local adaptation (Rocha *et al.* 2005; Momigliano *et al.* 2017). Improvements in methodology have further enabled the use of genome-wide polymorphism data to infer complex demographic histories and the relative influence of gene flow and historical processes on the genomic landscape. For example, in the marine environment this approach has been used in the European anchovy *Engraulis encrasicolus* (Le Moan *et al.* 2016), the Atlantic Salmon *Salmo salar* (Rougemont & Bernatchez 2018), and the corkscrew sea anemone *Bartholomea annulate* (Titus *et al.* 2019). One increasingly popular approach is demographic inference based on the computation of a joint allele frequency spectrum (JAFS) from genetic polymorphism data (Gutenkunst *et al.* 2009; Excoffier *et al.* 2013). This approach allows an estimation of several demographic parameters such as population sizes, migration rates and time intervals since specific events using a composite likelihood. Therefore, the role of historical events in the diversification and speciation of marine species can now be more accurately determined.

Rock lobsters (*Jasus* spp.) are a useful model to study the role of historical climatic variations and gene flow on divergence. The six extant *Jasus* lobster species (*J. caveorum*, *J. edwardsii*, *J. frontalis*, *J. lalandii*, *J. paulensis* and *J. tristani*) are distributed in a narrow latitudinal band (~25° to 47°; Fig. 1a) in the Southern

104 Hemisphere (Booth 2006) from 0 to 600 m (Holthuis 1991; Duhamel personal communication). These animals  
105 have a long pelagic larval duration (PLD; up to two years for *J. edwardsii*), with the potential for extensive  
106 dispersal (Bradford *et al.* 2015). Despite such a long PLD, all species have a restricted latitudinal distribution;  
107 for example, *J. caveorum* is only known from a single seamount in the eastern South Pacific Ocean (Webber &  
108 Booth 1995). Phylogenetic relationships between *Jasus* species have been investigated with a limited number  
109 of mtDNA markers (Brasher *et al.* 1992; Ovenden *et al.* 1997). Ovenden *et al.* (1997) identified a clade  
110 containing *J. edwardsii*, *J. lalandii* and *J. frontalis*, however, the relative branching order was not resolved by  
111 analysis of sequence variation in the cytochrome c oxidase subunit I (COI) and the 16S ribosomal RNA  
112 sequences. In addition, the species *J. tristani* and *J. paulensis*, which occur in islands and seamounts off the  
113 southern Atlantic and Indian Oceans, respectively, were hypothesized to have come into secondary contact  
114 during past glacial periods, resulting in low levels of mtDNA differentiation (Ovenden *et al.* 1997; Groeneveld  
115 *et al.* 2012). At the species level, population genetic studies have demonstrated a general pattern of low, yet  
116 often significant, differentiation (Ovenden *et al.* 1992; Matthee *et al.* 2007; Porobić *et al.* 2013; Thomas & Bell  
117 2013; Villacorta-Rath *et al.* 2016). Post-settlement selection and chaotic genetic patchiness, also described as  
118 a shifting, ephemeral genetic pattern, has also been observed in *J. edwardsii*, highlighting the uncertainties in  
119 predicting connectivity between populations of highly dispersive marine organisms (Villacorta-Rath *et al.*  
120 2018).

121         Although a few studies suggest a recent divergence between *Jasus* lineages (e.g. divergence within  
122 the *J. edwardsii* clade and within the *J. tristani*/*J. paulensis* clade may be 0.5 million years; Pollock 1990;  
123 Ovenden *et al.* 1997), relatively little attention has focused on investigating diversification processes in *Jasus*  
124 lobsters. Here we investigate speciation processes in all the extant lobster species of the genus *Jasus*. Given  
125 the potential for long distance dispersal, we expect that gene flow (i.e. secondary contact after divergence)  
126 between species are relatively common. Therefore, this study aims to determine if admixture/introgression  
127 has occurred between species, to investigate the genetic patterns associated with habitat structure  
128 (continental shelf or seamount/island) and to infer the demographic history of *Jasus* spp. pairs using genome-  
129 wide single nucleotide polymorphisms (SNP).

## Methods

### *Sampling, DNA extractions and sequencing*

Tissue samples of *Jasus* spp. were collected between 1995 and 2017 from 17 locations throughout the entire genus' range (Fig. 1a). A total of 375 samples were collected from 17 populations in total: *J. caveorum* (n=1), *J. edwardsii* (n=5), *J. frontalis* (n=1), *J. lalandii* (n=5), *J. paulensis* (n=2) and *J. tristani* (n=3). Tissue was stored in 70% ethanol before processing. Total genomic DNA of *J. caveorum* historic samples (i.e. collected in 1995) was extracted using the QIAamp DNA Micro Kit (Qiagen) according to the manufacturer's instruction. The remaining tissue samples were extracted using NucleoMag® Tissue (Macherey-Nagel) following to the manufacturer's instructions.

Library preparation and sequencing was conducted by Diversity Arrays Technology, Canberra, Australia and followed standard protocols of DArTseq™ genotyping technology (Kilian *et al.* 2012). Briefly, approximately 100 ng (2 µL) of each sample was digested with the restriction enzymes PstI and SphI, and unique barcode sequences simultaneously ligated onto the ends of each resulting fragment as per Kilian *et al.* 2012. The PstI-compatible adapter included an Illumina flow-cell attachment sequence, a primer sequence and unique barcode, with the reverse SphI-compatible adaptor contained in the flow-cell attachment region. Size selection was performed using a competitive PCR, where longer fragments and those without both cut sites were excluded. A minimum of 15% random technical sequencing replicates were included for downstream quality control. Each sample with fragments containing both PstI and SphI cut sites was amplified in independent PCR reactions using the following conditions: 94°C for 1 min then 30 cycles of 94 °C for 20 s, 58 °C for 30 s, 72 °C for 45 s, and 72 °C for 7 min. Samples were checked visually on an agarose gel to ensure complete digestion and uniform range of fragment sizes. Using approximately 10 µL of each sample, samples were sequenced on a single flow-cell lane on the Illumina HiSeq2500 for 77 cycles.

### *De novo assembly and variant calling*

Libraries were demultiplexed and reads were filtered for overall quality (`-c`, `-q` and `-r` options) using *process\_radtags* in STACKS v.2.0b9 (Catchen *et al.* 2013). The Stacks pipeline *denovo\_map.pl* was executed to run each of the Stacks modules individually (*ustacks*, *cstacks*, *sstacks* and *populations*). To optimise the *denovo* assembly we tested a range of parameters, including *m* (minimum stack depth) of 3, 5 and 10 and *M* (distance allowed between stacks) and *n* (distance allowed between catalog loci) from 1 to 9, as recommended by Rochette & Catchen (2017) and Paris *et al.* (2017). The parameter test showed that *M*=3 provided a balance between obtaining true polymorphism and introducing sequencing error (i.e. the number of widely shared loci plateaued at about *M*=3) and that *M*=3 was sufficient to stabilize the proportions of loci with 1–5 SNPs (Fig. S1). The high coverage with the value of *m*=3 (64x) and consistent results with *m*=3 to *m*=10 imply a true biological signal (Fig. S1). As *m*=3 also performs well for a broad range of data sets (Paris *et al.* 2017; Rochette & Catchen 2017) we retained *m*=3 for the main analysis. The formation of loci was allowed with a maximum of two nucleotides between stacks (*M* = 3) and a minimum stack depth of three (*m* = 3) among reads for accurate calling (*ustacks* module). Reads were aligned *de novo* with each other, and a catalogue of putative RAD tags was created (*cstacks* module). Putative loci were searched against the catalog (*sstacks* module) and further filtering was then conducted in the *populations* module.

Retained SNPs were present in at least 70% of samples within each species, were detected in all species, had a rare allele frequency of at least 2% (to minimize sequencing errors and exclude singletons; Linck & Battey 2019) and had no more than 2 alleles detected. Potential paralogs were excluded by removing markers with heterozygosity > 0.50 within samples and analyses were restricted to one random SNP per locus (using `--write_random_snp`). These filtering steps aimed to exclude as many SNPs as was possible with genotyping errors and missing data.

### *Genetic diversity and population structure*

Allelic richness, pairwise  $F_{ST}$  values and respective p-values were estimated using *hierfstat* package in R (Goudet 2005). The R package *adegenet* was used to estimate observed and expected heterozygosity and for discriminant analyses of principal components (DAPC) and membership probability plots (Jombart 2008).



185 DAPC was used on individual genotypes in a multivariate analysis to determine the best number of genetic  
186 clusters (K) to retain by running the function *find.clusters()*. Five clusters, five discriminant functions and two  
187 principal components (PC) were retained. Inbreeding coefficients were estimated using GenoDive v3  
188 (Meirmans & Van Tienderen 2004). Outlier analyses were conducted in BayeScan to look for signatures of  
189 selection. Prior odds were set to 100 to minimize chances of false positives with 5,000 pilot runs, followed by  
190 100,000 iterations (5,000 samples, a thinning interval of 10, and a burn-in of 50,000).

191

#### 192 *Environmental data collection and analyses*

193

194 Initially, 13 environmental variables were obtained from Bio-Oracle (Assis *et al.* 2018; Table S1). Only  
195 uncorrelated variables ( $r < 0.6$ ) were retained in order to avoid testing strongly interdependent models and to  
196 effectively estimate the relative importance of different factors. This resulted in seven layers (surface and  
197 benthic temperature mean, surface salinity, surface and benthic current velocity, benthic iron and surface  
198 phytoplankton). Linear mixed-effects models were used to examine the association of geographic distance  
199 (estimated as the shortest path distance in the ocean) with patterns of genetic differentiation (measured as  
200 pairwise  $F_{ST}$  values), using the R package lme4 (Bates *et al.* 2015). Species was incorporated as a random effect  
201 to control for specific demographic histories. We tested associations for all (17) populations and for 15  
202 populations only (i.e. removed the Pacific species *J. frontalis* and *J. caveorum*) as only one location per species  
203 was sampled.

204 Redundancy analysis (RDA; Forester *et al.* 2018) was used to investigate genotype-environment  
205 associations using the R package vegan (Oksanen *et al.* 2019). RDA is a two-step analysis in which genetic and  
206 environmental data are first analysed using multivariate linear regression, producing a matrix of fitted values  
207 (i.e. constrained axes) and then a principal component analysis (PCA) of the fitted values produces canonical  
208 axes (i.e. unconstrained axes), which are linear combinations of the predictors. Significance was assessed using  
209 a permutation test (999 permutations) for redundancy analysis using the function *anova.cca()*.

210

#### 211 *Relationships among lineages*

212

213         The program TREEMIX v1.12 (Pickrell & Pritchard 2012) was used to further investigate historical  
214 relationships among lineages. A maximum-likelihood (ML) phylogeny was first inferred and then single  
215 migration events between branches were sequentially added to determine whether migration/admixture  
216 events improve the likelihood fit. To formally test for admixture between *Jasus* spp., the three-population test  
217 (Reich *et al.* 2009) included with TREEMIX was used. In this test, the  $f_3(X; A, B)$  statistic is negative when a  
218 population X does not form a simple tree with populations A and B, but rather may be a mixture of A and B.  
219 As composite likelihood cannot be used directly for formal tests for significance, confidence in individual  
220 migration events was estimated using a resampling approach. Therefore “significant” values indicate that the  
221 hypothesized migration event significantly improves the fit to the data.

222

#### 223 *Demographic modelling*

224

225         Previous analysis suggests evidence of admixture between species pairs, and so we tested several  
226 hypothesis of divergence modes, aiming to identify speciation events through time, for each closely related  
227 pair of species: *J. caveorum* - *J. frontalis*, *J. edwardsii* - *J. lalandii* and *J. tristani* - *J. paulensis*. The species pairs  
228 were selected based on their genetic and morphological relationships (Holthuis & Sivertsen 1967; George &  
229 Kensler 1970; Brasher *et al.* 1992; Ovenden *et al.* 1997; Groeneveld *et al.* 2012; this study). A set of simple  
230 scenarios (i.e. Divergence in Strict Isolation and Isolation-with-Migration) was chosen and complexity was  
231 added to these models to take into account specific aspects of divergence between these species. Repeated  
232 periods of secondary contact interrupted by isolation were tested (i.e. divergence with Ancient Migration and  
233 divergence with Secondary Contact) as species have a long larvae duration and therefore gene flow during  
234 divergence is likely. Finally, recent expansion (prefix ‘ex’) was also tested to allow for demographic events  
235 following the last glacial maximum (LGM). For each pair, 12 models were built representing alternative modes  
236 of divergence considering possible scenarios (Fig S4): (SI) Strict Isolation; (SIex) Strict Isolation with a recent  
237 expansion/contraction event; (IM) Isolation-with-Migration; (IMex) Isolation-with-Migration with a recent  
238 expansion/contraction event; (AM) Ancient Migration with an ancient gene flow event but recent isolation;

239 (AMex) Ancient Migration with an ancient gene flow event but recent isolation and with a recent  
 240 expansion/contraction event; (SC) Secondary Contact with a recent gene flow event after past isolation; (SCex)  
 241 Secondary Contact with a recent gene flow event after past isolation and with a recent expansion/contraction  
 242 event; (PAM) Repeated Ancient Migration with two ancient gene flow events but recent isolation; (PAMex)  
 243 Repeated Ancient Migration with two ancient gene flow events but recent isolation and with a recent  
 244 expansion/contraction event; (PSC) Repeated Secondary Contact with two recent gene flow events after past  
 245 isolation; (PSCex) Repeated Secondary Contact with two recent gene flow events after past isolation and with  
 246 a recent expansion/contraction event. All models were implemented allowing for asymmetric migration rates  
 247 ( $m_{12}$ ,  $m_{21}$ ).

248 Demographic inference was performed using the diffusion approximation method implemented in the  
 249 software *daði* (Gutenkunst *et al.* 2009). The function *vcf2dadi* in the R package *radiator* (Gosselin 2017) was  
 250 used to create *daði* SNP input files. We used the folded joint site frequency spectrum (JSFS) for model selection  
 251 because the closest out-group (*Sagmariasus verreauxi*) was too distant (diverged around 11 Mya; Ovenden *et al.*  
 252 1997), which resulted in a highly reduced number of orientable polymorphisms. To address the impact of  
 253 missing data in generating JSFS we have projected all spectra down to half of the samples per population (per  
 254 species pair), as recommended by Gutenkunst *et al.* (2009). As there was a constant reduction in the number  
 255 of segregating sites (i.e. the projection did not maximise the number of segregating sites; Table S3) we have  
 256 used all samples for the inference of the final JSFS.

257 In total, 12 models were tested per species pair, fitted with the observed joint site frequency spectrum  
 258 (SFS) using 20 replicate runs per model and the best model was retained (Fig. S3). The Akaike information  
 259 criterion (AIC) was used to perform comparisons among models (Sakamoto *et al.* 1986).

260 To compare among nested models of increasing complexity and address over-parametrization issues  
 261 we used the comparative framework of Tine *et al.* (2014) by penalizing models which contain more  
 262 parameters. For each species pair, a score was estimated for each model using:

$$263 \text{ Score} = \frac{(\Delta_{\max} - \Delta \text{AIC}_i)}{\Delta_{\max}} \quad (1)$$

265

266 where,  $\Delta_{\max}$  corresponds to the difference in AIC between the worst and the best performing model ( $\Delta_{\max} =$   
 267  $AIC_{\max} - AIC_{\min}$ ) and  $\Delta AIC_i = AIC_i - AIC_{\min}$ . Therefore, the worst model has a score of 0 and the best model has a  
 268 score of 1. To evaluate the relative probabilities of the different models within each species pair, Akaike  
 269 weights ( $W_{AIC}$ ) were also calculated following:

270

$$271 \quad W_{AIC} = \frac{e^{\frac{-(\Delta AIC_i)}{2}}}{\sum_{i=1}^R e^{\frac{-(\Delta AIC_i)}{2}}} \quad (2)$$

272

273 where R corresponds to the total number of models considered (R=12).

274 Demographic parameters were converted into indicative biologically units, given the missing crucial  
 275 information about mutation rate per generation in *Jasus* spp. The ancestral effective population size ( $N_{\text{ref}}$ )  
 276 before split for each species pair was estimated following:

277

$$278 \quad N_{\text{ref}} = \frac{\theta}{4L\mu} \quad (3)$$

279

280 with  $\theta$  being the optimal multiplicative scaling factor,  $\mu$  the mutation rate (fixed at  $8 \times 10^{-8}$  mutations per site  
 281 per generation; Obbard *et al.* 2012) and L the effective length of the genome explored:

282

$$283 \quad L = \frac{zy73}{x} \quad (4)$$

284

285 where x is the number of SNPs originally detected from y RAD-tags of 73 bp present in the initial data set, and  
 286 z the number of SNPs retained, following Rougeux *et al.* (2017). Estimated units in  $2N_{\text{ref}}$  were converted to  
 287 years assuming a generation time of 10 years (Pecl *et al.* 2009). Estimated migration rates were divided by  
 288  $2N_{\text{ref}}$  to obtain the proportion of migrants in every generation.

289

290

## 291 **Results**

### 292 *Genetic diversity and population structure*

293  
294  
295  
296  
297  
298  
299  
300  
301  
302  
303  
304  
305  
306  
307  
308  
309

Sequencing yielded a total of 1,501,921,855 quality-trimmed sequencing reads, providing an average depth of coverage per individual over all SNPs of 58.9x. After applying the different filtering steps, 2,596 SNPs common to all species were retained for subsequent analyses, which had an average depth of coverage of 64x (mean coverage per individual over all SNPs). The lowest values of observed heterozygosity, expected heterozygosity, and allelic richness were observed for *J. caveorum* and *J. lalandii* had the highest inbreeding coefficients (0.178). The highest values of allelic richness were observed for *J. lalandii* (Table 1). The highest pairwise  $F_{ST}$  values were observed for *J. tristani* – *J. caveorum* and *J. paulensis* – *J. caveorum* ( $F_{ST}$  = 0.463 and  $F_{ST}$  = 0.436, respectively,  $p < 0.05$ ), while the lowest values were observed for *J. tristani* – *J. paulensis* ( $F_{ST}$  = 0.022,  $p < 0.01$ ; Table 2).

**Table 1** Summary statistics of genetic diversity per species using 2,596 SNPs.  $H_O$ : observed heterozygosity,  $H_E$ : expected heterozygosity,  $F_{IS}$ : inbreeding coefficient,  $A_R$ : allelic richness

Species	Sample size	$H_O$	$H_E$	$F_{IS}$	$A_R$
<i>J. caveorum</i>	11	0.012	0.012	0.094	1.04
<i>J. frontalis</i>	53	0.064	0.065	0.026	1.32
<i>J. tristani</i>	41	0.092	0.104	0.127	1.31
<i>J. lalandii</i>	129	0.086	0.104	0.178	1.60
<i>J. paulensis</i>	49	0.087	0.103	0.159	1.31
<i>J. edwardsii</i>	92	0.084	0.100	0.166	1.34
375					

**Table 2** Pairwise  $F_{ST}$  values (below diagonal) and corresponding p-values (above diagonal) estimated using *hierfstat* package in R.

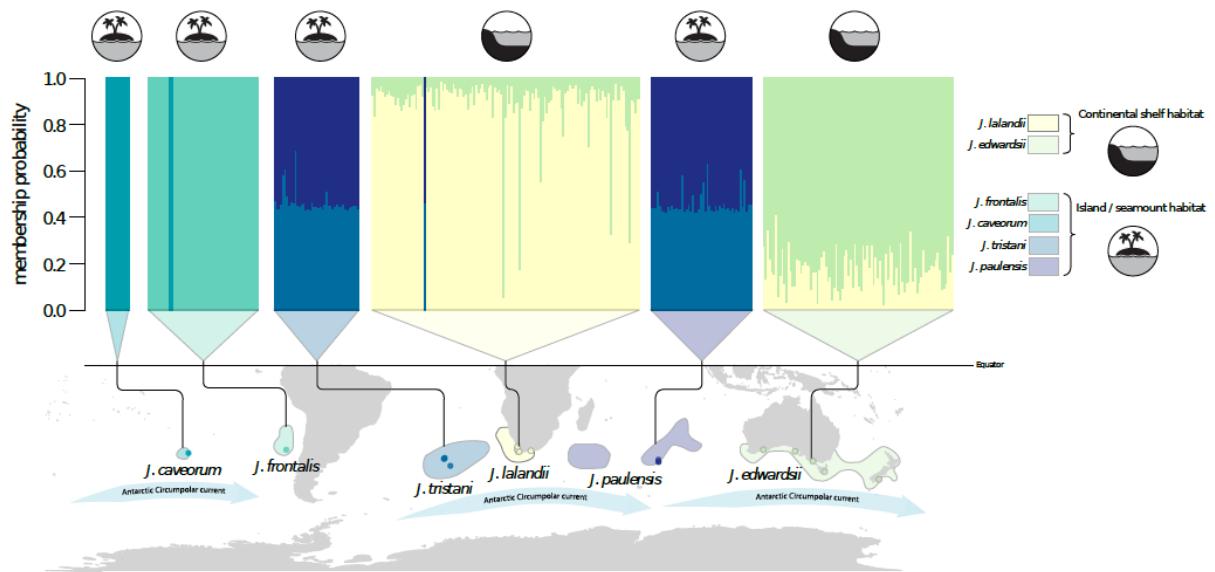
	<i>J. caveorum</i>	<i>J. frontalis</i>	<i>J. tristani</i>	<i>J. lalandii</i>	<i>J. paulensis</i>	<i>J. edwardsii</i>
<i>J. caveorum</i>	0	0.010	0.013	0.010	0.011	0.012
<i>J. frontalis</i>	0.081	0	0.007	0.005	0.006	0.007
<i>J. tristani</i>	0.463	0.206	0	0.007	0.008	0.009
<i>J. lalandii</i>	0.305	0.137	0.387	0	0.006	0.007
<i>J. paulensis</i>	0.436	0.229	0.022	0.408	0	0.007
<i>J. edwardsii</i>	0.413	0.106	0.441	0.230	0.452	0

310 No signatures of selection were detected by the outlier detection analyses (Fig. S2). Lobster species  
311 were grouped into three main clusters by discriminant analyses of principal components when using 2 PCs  
312 (52.3% variation) (Fig. 1b). There was evidence of admixture, in particular between *J. paulensis* - *J. tristani* in  
313 the membership probability plot, the DAPC results and pairwise  $F_{ST}$  values (Fig. 1a, b). The first DAPC axis (LD1)  
314 explained 29.9% of the variation and highlighted the divergence between habitat structure (i.e. *J. edwardsii*  
315 and *J. lalandii* vs. remaining species; Fig. S3a), while the second DAPC axis (LD2), which explained 22.4% of the  
316 variation, showed three main clusters and highlighted the differences between *J. paulensis* and *J. tristani* and  
317 the remaining species (Fig. S3b).

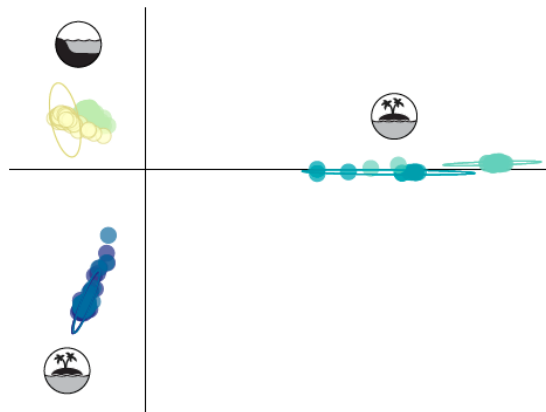
318

319

a)



b)



c)

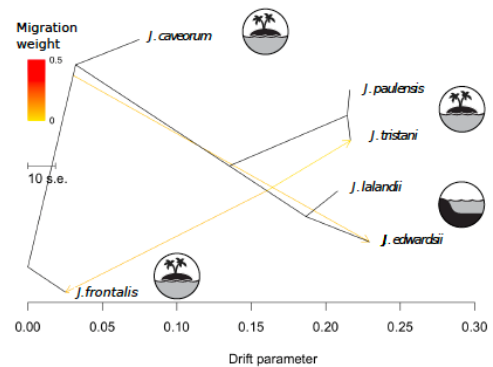


**Fig. 1.** a) Sample locations, approximate distribution range of *Jasus* spp. (adapted from Booth, 2006) and membership probability plot using two principal components. b) Discriminant analyses of principal components (DAPC) of *Jasus* spp. using two principal components (explaining a total of 52.3% variation, with the first horizontal axis explaining 29.9% and the second vertical axis explaining 22.4% of the variation). c) TreeMix results showing three ancestral admixture events.

### Genotype-environment associations

Genetic variation ( $F_{ST}$ ) between rock lobster species was significantly correlated with benthic temperature ( $p < 0.001$  for 17 populations and  $p < 0.01$  for 15 populations) and benthic current velocity

( $p < 0.001$ ), when controlling for the effects of geographic distance. Models including geographic distance as the only predictor of genetic variation were also significant ( $p < 0.05$  for 17 populations and  $p < 0.001$  for 15 populations; Table 3).

All seven environmental variables explained 18% of the variation in rock lobster species ( $p < 0.001$ ) when using the constrained ordination in RDA analyses. All values of the variance inflation factors were below five, indicating that multicollinearity among the predictor variables is not inflating the model. The first five constrained axes were significant in explaining the genetic variation between species (each explaining 53.3%, 25.3%, 12%, 5.2% and 2.2%, respectively;  $p < 0.001$ ; Fig. 2). Genetic variation of *J. caveorum* and *J. frontalis* was associated with higher surface temperature, while *J. paulensis* and *J. tristani* were associated with lower surface temperature. *J. edwardsii* and *J. lalandii* were associated with higher benthic temperature, benthic current velocity and benthic iron. Finally, *J. lalandii* was associated with higher surface phytoplankton, while *J. edwardsii* was associated with higher surface current velocity (Fig. 2).

**Table 3** Summary of the mixed effects model analyses for all species (17 populations) and for *J. tristani*, *J. lalandii*, *J. paulensis* and *J. edwardsii* only (15 populations) using  $F_{ST}$  as a measure of genetic differentiation (dependent variable) and species as a random effect. GeoDist: geographic distance (km); SurfTemp and BenTemp: Surface and benthic temperature ( $^{\circ}\text{C}$ ); SurfSal: Surface salinity (PSS); SurfCurren and BenCurren: Surface and benthic current velocity ( $\text{m.s}^{-1}$ ); BenIron: Benthic dissolved iron ( $\text{mmol.m}^{-3}$ ); SurfPhyto: surface phytoplankton ( $\text{mmol.m}^{-3}$ ).

	All species, 17 populations			Four species, 15 populations		
Fixed effects	REML	p-value	AIC	REML	p-value	AIC
<b>GeoDist</b>	<b>131.9</b>	<b>&lt;0.050</b>	<b>139.9</b>	<b>94.1</b>	<b>&lt;0.001</b>	<b>102.1</b>
GeoDist + SurfTemp	137.7	0.336	147.7	100.2	0.464	110.1
<b>GeoDist + BenTemp</b>	<b>110.9</b>	<b>&lt;0.001</b>	<b>120.9</b>	<b>93.7</b>	<b>&lt;0.010</b>	<b>103.7</b>
GeoDist + SurfSal	133.9	0.124	143.9	97.2	0.274	107.2
GeoDist + SurfCurren	130.2	0.251	140.2	91.4	0.139	101.4
<b>GeoDist + BenCurren</b>	<b>117.7</b>	<b>&lt;0.001</b>	<b>127.7</b>	<b>75.0</b>	<b>&lt;0.001</b>	<b>85.0</b>
GeoDist + BenIron	125.6	0.921	135.6	86.8	0.332	96.8
GeoDist + SurfPhyto	137.0	0.097	147.0	98.1	0.059	108.1



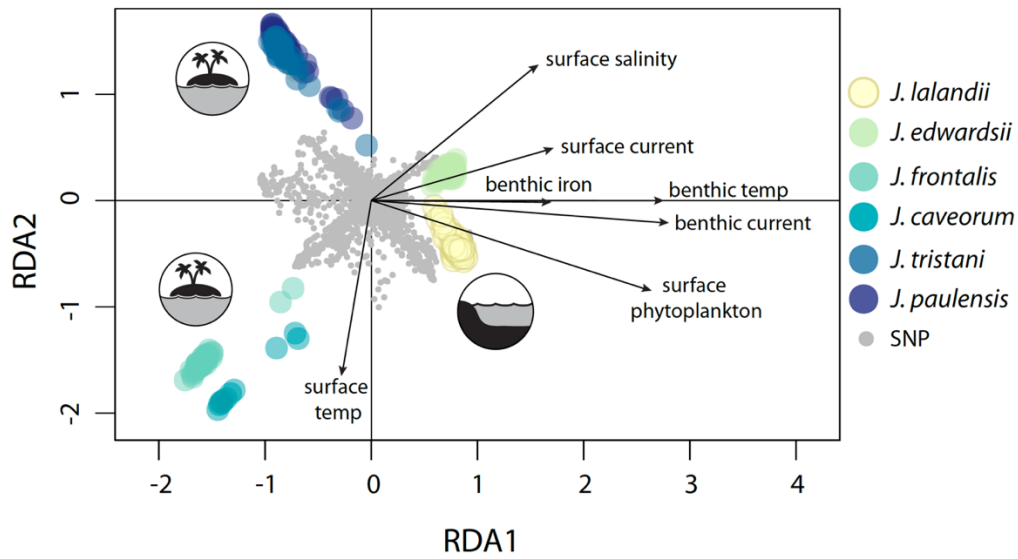


**Fig. 2.** Ordination plot of redundancy analysis (RDA) of *Jasus* spp. The vectors are the environmental predictors (see Table 3 for a detailed description).

### Relationships among lineages

Results from TREEMIX identified three ancestral events of admixture (Fig. 1c). However, from the three-population test of admixture, only two  $f_3$  values were negative with associated Z-scores  $< -0.6$ , indicating evidence that *J. tristani* does not form a simple tree with *J. paulensis*, *J. lalandii* and *J. edwardsii*, but rather may be a mixture of these (Table S2, Supporting information). Therefore, the three-population test supported the ancestral event of admixture detected by TREEMIX from the most recent common ancestor (MRCA) of *J. lalandii* and *J. edwardsii* to *J. tristani*. The genetic relationships among species inferred by TREEMIX revealed similar patterns to the genetic differentiation analyses, clearly separating species pairs *J. lalandii*–*J. edwardsii*, *J. paulensis*–*J. tristani* and *J. caveorum*–*J. frontalis* (Fig. 1c).

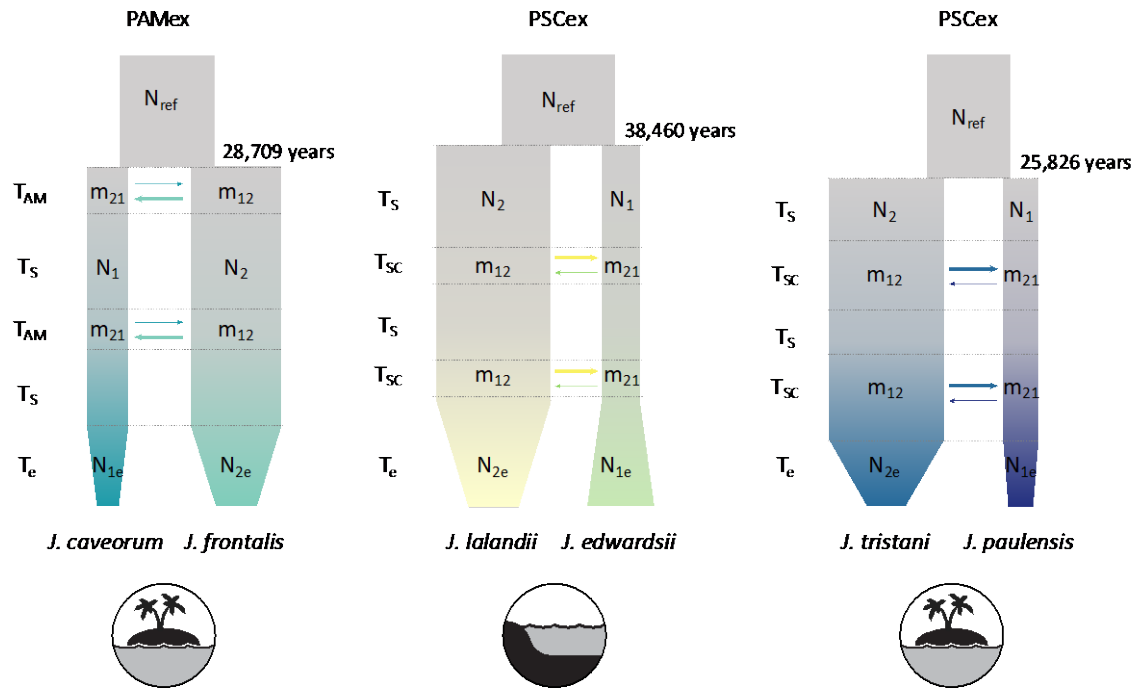
### Demographic modelling

The models for secondary contact (SC) and repeated secondary contact (PSC) provided better fits to the data with good predictions of the joint site frequency spectrum (JSFS) asymmetry for the *J. paulensis*–*J. tristani* and *J. edwardsii*–*J. lalandii* pairs while ancient migration (AM), repeated ancient migration (PAM) and

strict isolation (SI) had better support for the *J. caveorum* – *J. frontalis* pair (Table S4, Fig. S4). Incorporating population expansion events improved the fit of PSC models for all species pairs but there was not a clear pattern for PAM models. In contrast, the strict isolation (SI) and ancient migration (AM, PAM) models were weakly supported for the *J. paulensis* – *J. tristani* and *J. edwardsii* – *J. lalandii* pairs while the secondary contact models (SC, PSC) were weakly supported for the *J. caveorum* – *J. frontalis* pair (Table S4, Fig. S3).

Asymmetries in gene flow with ratios of  $m_{21}/m_{12}$  indicated a stronger migration from population two to population one in all species pairs, and the lower proportion of migrants was observed for the *J. edwardsii* – *J. lalandii* pair (Fig. 3, Table 4). Detailed results for demographic inferences are provided in Fig. 3, Table 4, Fig. S4, Fig. S5, Fig. S6 and Table S4 (supporting information).

The best supported model for the *J. paulensis* – *J. tristani* pair was PSCex (Table S4). Within this model, total divergence time between species was approximately  $25,826 \pm 6,286$  years ago (Table 4). The period without contact was approximately 5.4 times longer than the period with secondary contact. The best supported model for the *J. edwardsii* – *J. lalandii* pair was PSCex (Table S4). Total divergence time between *J. edwardsii* and *J. lalandii* was approximately  $38,460 \pm 12,242$  years ago (Table 4). The period without contact was approximately 38.8 times longer than the period with secondary contact. Finally, the best supported model for the *J. caveorum* – *J. frontalis* pair was PAMex (Table S4). Within this model, total divergence time between species was approximately  $28,709 \pm 12,674$  years (Table 4) and the period without contact was approximately 8.1 times longer than the period with ancient migration. Therefore, divergence times with errors overlap across the three species pairs and was estimated to be between 19,540 and 32,112 years for *J. paulensis* – *J. tristani*, 26,218 and 50,702 years for *J. edwardsii* – *J. lalandii* and 16,035 and 41,383 years for *J. caveorum* – *J. frontalis*.



401

402

403

404

405

406

407

408

409

410

411

**Fig. 3.** Representation of the best demographic model for each species pair; *J. caveorum* – *J. frontalis*: ancient migration with two periods of ancient gene flow and recent population contraction (PAMex); *J. lalandii* – *J. edwardsii* and *J. tristani* – *J. paulensis*: secondary contact with two periods of contact and recent population expansion/contraction (PSCex). Asymmetric migration rates ( $m_{21}$  and  $m_{12}$ ) are represented by the arrows with higher rates of migration from population two to population one for all species pairs (thicker lines in arrows). Width of the boxes represent sizes of the ancestral population ( $N_{ref}$ ), population sizes before expansion/contraction ( $N_1$ ,  $N_2$ ) and population sizes after expansion/contraction ( $N_{1e}$ ,  $N_{2e}$ ).  $T_s$  is the time of divergence in strict isolation,  $T_{SC/AM}$  the time of secondary contact or ancient migration and  $T_e$  the time of expansion.

**Table 4.** Parameters estimates for the best model of each species pair with standard deviation. *J. paulensis* – *J. tristani*: secondary contact with two periods of contact and recent population expansion (PSCex); *J. edwardsii* – *J. lalandii*: secondary contact and recent population expansion (SCex); *J. caveorum* – *J. frontalis*: ancient migration with two periods of ancient gene flow and recent population contraction (PAMex).

Species group	1: <i>J. paulensis</i> , 2: <i>J. tristani</i>	1: <i>J. edwardsii</i> , 2: <i>J. lalandii</i>	1: <i>J. caveorum</i> , 2: <i>J. frontalis</i>
<b>Best Model</b>	PSCex	PSCex	PAMex
<b>K</b>	9	9	9
<b>N<sub>ref</sub></b>	43.96	85.64	64.19
<b>N<sub>1</sub></b>	3.50 ± 0.84	1.50 ± 0.25	1.30 ± 0.35
<b>N<sub>2</sub></b>	49.67 ± 19.38	41.01 ± 15.61	19.19 ± 9.09
<b>N<sub>1e</sub></b>	0.67 ± 0.16	2.44 ± 0.41	0.05 ± 0.24
<b>N<sub>2e</sub></b>	2.52 ± 0.53	1.28 ± 0.34	0.20 ± 0.23
<b>m<sub>12</sub></b>	11.00 ± 3.77	1.77 ± 0.23	7.71 ± 2.33
<b>m<sub>21</sub></b>	2.59 ± 2.22	0.09 ± 0.16	1.99 ± 0.36
<b>T<sub>S</sub></b>	11.94 ± 2.67	10.66 ± 3.37	9.74 ± 4.48
<b>T<sub>SC/AM</sub></b>	2.20 ± 0.70	0.27 ± 0.10	1.20 ± 0.19
<b>T<sub>e</sub></b>	0.51 ± 0.20	0.29 ± 0.11	0.24 ± 0.27
<b>T<sub>total</sub></b>	29.29 ± 7.15	22.46 ± 7.15	22.36 ± 9.87
<b>*m<sub>12</sub></b>	0.12 ± 0.04	0.01 ± 0.001	0.06 ± 0.02
<b>*m<sub>21</sub></b>	0.03 ± 0.03	0.00 ± 0.00	0.01 ± 0.00
<b>*T<sub>S</sub></b>	10,524 ± 2,346	18,258 ± 5,769	12,507 ± 5,746
<b>*T<sub>SC/AM</sub></b>	1,941 ± 618	470 ± 167	1,541 ± 239
<b>*T<sub>e</sub></b>	447 ± 179	503 ± 185	306 ± 352
<b>*T<sub>total</sub></b>	25,826 ± 6,286	38,460 ± 12,242	28,709 ± 12,674

K: The number of free parameters in the model

N<sub>ref</sub>: The effective size of the ancestral population before the split

N<sub>1</sub>: The effective size of population 1 before expansion in units of 2N<sub>ref</sub> generations

N<sub>2</sub>: The effective size of population 2 before expansion in units of 2N<sub>ref</sub> generations

N<sub>1e</sub>: The effective size of population 1 after expansion in units of 2N<sub>ref</sub> generations

N<sub>2e</sub>: The effective size of population 2 after expansion in units of 2N<sub>ref</sub> generations

m<sub>12</sub>: The neutral movement of genes from population 2 to population 1 in units of 2N<sub>ref</sub> generations

m<sub>21</sub>: The neutral movement of genes from population 1 to population 2 in units of 2N<sub>ref</sub> generations

T<sub>S</sub>: The time of divergence in strict isolation in units of 2N<sub>ref</sub> generations

T<sub>SC/AM</sub>: The time of secondary contact/ancient migration in units of 2N<sub>ref</sub> generations

T<sub>e</sub>: The time of expansion in units of 2N<sub>ref</sub> generations

T<sub>total</sub>: The total time since the split in units of 2N<sub>ref</sub> generations

\*m<sub>12</sub>: The proportion of migrants per generation from population 2 to population 1

\*m<sub>21</sub>: The proportion of migrants per generation from population 1 to population 1

\*T<sub>S</sub>: The time of divergence in strict isolation in units of numbers of years

\*T<sub>SC/AM</sub>: The time of secondary contact/ancient migration in units of numbers of years

\*T<sub>e</sub>: The time of expansion in units of numbers of years

\*T<sub>total</sub>: The total time since the split in units of numbers of years

## Discussion

Here we investigated genome-wide divergence and introgression patterns in all extant species of rock lobsters (*Jasus* spp.) for the first time. Genetic differentiation patterns revealed the effects of geographical isolation and the environment (i.e. habitat structure), with benthic temperature being the environmental variable that explained most of the genetic differentiation ( $F_{ST}$ ) while controlling for the effects of geographic distance. Closely related species pairs were identified and for all three species pairs we detected recent divergence and multiple introgression events (gene flow) since first divergence.

### Drivers of speciation

In our study, the Eastern Pacific species pair (*J. caveorum* and *J. frontalis*) were genetically more differentiated from the remaining species. Therefore, geographic distance and reduced ocean current velocity in the Southern Pacific might have driven the differentiation between the Eastern Pacific and the remaining *Jasus* species. On the other hand, the main driver of differentiation between the other species pairs, *J. tristani* - *J. paulensis* and *J. lalandii* - *J. edwardsii*, was habitat structure. Species that were associated with the same habitat structure (continental shelf or seamount/island) were genetically more closely related to each other than to species from the alternate habitat, despite these habitat types being geographically interspersed. For example, *J. edwardsii* and *J. lalandii* (associated with continental shelf habitat) were genetically more similar to each other ( $F_{ST}=0.230$ ), as were *J. tristani* and *J. paulensis* (from island/seamount habitat;  $F_{ST}=0.022$ ). Yet *J. lalandii* is geographically much closer to *J. tristani* ( $F_{ST}=0.387$ ) and *J. paulensis* ( $F_{ST}=0.408$ ) than it is to *J. edwardsii* (Fig. 1). It is important to note that these results must be taken with caution as sample size is necessarily limited. Although connectivity is possible between these habitats given the high larval dispersal potential (indeed, *J. lalandii* larvae have been found in the southwest Indian Ocean as far east as Amsterdam Island, adjacent to the *J. paulensis* habitat (Booth & Ovenden 2000)), species appear to be adapted to local environmental conditions.

Our results suggest that benthic temperature is associated with the differentiation between species from island/seamount and continental shelf habitats. Benthic temperature explained most of the genetic

446 differentiation ( $F_{ST}$ ) while controlling for the effects of geographic distance, and *J. edwardsii* and *J. lalandii*  
447 were associated with higher mean benthic temperatures. Temperature is important for regulating the rate of  
448 embryological development in lobsters (Phillips 2013) and thermal adaptation has been detected in American  
449 lobster *Homarus americanus* (Benestan *et al.* 2016). Therefore, sea temperature could limit reproduction  
450 between populations of *Jasus* spp. adapted to local benthic temperatures.

451 Other factors may have also played a role in isolating locally adapted populations/species despite  
452 potential for long distance dispersal. Pollock (1990) noted that genetic differentiation between *Jasus* species  
453 may have been caused by interruptions of gene flow between populations as a result of topographic forcing  
454 of ocean currents by shoaling ridges, rises and island/seamount chains. For example, larvae may be retained  
455 within permanent eddies found offshore (Chiswell & Booth 1999), which may also be limiting dispersal  
456 between habitats (continental shelf and islands/seamounts). In addition, despite *Jasus* larvae being weak  
457 horizontal swimmers, they can migrate vertically in the water column (Booth 1994) and therefore can use this  
458 to their advantage to avoid being transported offshore or towards unsuitable habitat. Differential settlement  
459 trends between species can also play a role in isolating locally adapted populations/species. It has been shown  
460 that during the post-larval or puerulus stage, *J. edwardsii* are able to recognize environmental cues such as  
461 chemical, acoustic and substrate cues, and increase settlement success in suitable habitats (Stanley *et al.* 2015;  
462 Hinojosa *et al.* 2016, 2018). Therefore, a combination of factors can drive divergence between *Jasus* spp.  
463 regardless of geographic location.

464 Divergence times within species pairs estimated by the best fitting demographic models in this study  
465 overlap across all species comparisons (from  $38,460 \pm 12,242$  to  $25,826 \pm 6,286$  years ago), suggesting that  
466 global changes in environmental conditions might have driven initial divergence across all species pairs. Such  
467 a scenario closely matches the recent radiations inferred for the synonymous genera of perciform fishes  
468 *Nemadactylus* and *Acantholatris*, which overlap in distribution with *Jasus* spp. and also have a long pelagic  
469 larval stage of 7-12 months (Burridge 1999). Therefore, we hypothesise that global changes in environmental  
470 conditions have similarly shaped the divergence patterns of these marine species complexes.

Decreasing global mean sea level and a change in the Southern Ocean (SO) barotropic stream function could have contributed to the co-occurring patterns of divergence among species pairs. The SO barotropic stream function is a measure of the strength of the Antarctic Circumpolar current (ACC), which drives currents in a predominately clockwise direction around Antarctica linking the major basins of the world. A significant change in the direction of the SO barotropic stream function occurred around 28,500 years ago (Fogwill *et al.* 2015; Fig 5e and f therein), which coincides with the expansion of Antarctic sea ice and the divergence period (within species pairs) estimated in our study (Fig. 4).

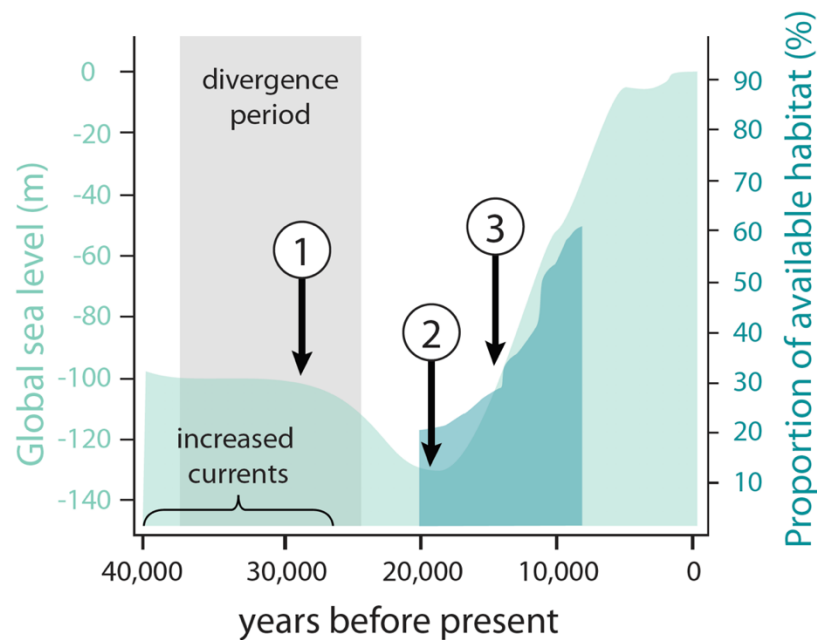


**Fig. 4.** Changes in global sea level (light green, adapted from Huybrechts 2002) and global mean proportion of available habitat in the benthic photic zone, from 0 to 65 metres (dark green, Schaaf 1996) relative to present day. 1) Antarctic sea ice expands around 28,500 years ago (Fogwill *et al.* 2015); 2) The end of the last glacial maximum (around 19,000 years ago; Clark *et al.* 2009); 3) West Antarctic Ice Sheet deglaciation (around 14,500 years ago; Clark *et al.* 2009). Divergence period corresponds to the initial divergence period between species pairs estimated from the demographic inference in this study.

## Secondary contact

In our study, the best fitting demographic models showed that for all species pairs the periods of isolation were longer than the periods of gene flow after divergence occurred. Past periods of isolation were

491 estimated to be between 5- and 39-fold longer than periods of gene flow for the *J. paulensis* – *J. tristani* pair  
492 and *J. edwardsii* – *J. lalandii*, respectively. The genetic structure observed reflects these demographic history  
493 characteristics, as the *J. paulensis* – *J. tristani* pair showed more distinct signatures of admixture than the *J.*  
494 *edwardsii* – *J. lalandii* pair. The best fitting demographic models also showed repeated periods of isolation  
495 followed by secondary contact for all species pairs. These patterns likely result from the impact of Quaternary  
496 climatic oscillations on *Jasus* populations, which are known to have promoted retreats towards lower latitudes  
497 during glacial periods (e.g. Kenchington *et al.* 2009; Le Moan *et al.* 2016; Jenkins *et al.* 2019) and thereby  
498 created new opportunities for isolation/contact during transition to interglacial periods.

499         During the last glacial maxima (LGM) about 19,000-22,000 years ago, temperature and sea levels  
500 reached minimum values (Clark *et al.* 2009). Low temperatures likely drove a northward shift in the  
501 distribution of species as they tracked their thermal optima. A more northerly distribution of *J. lalandii* and *J.*  
502 *edwardsii* than the present day, for example, could result in a reduction in connectivity between these species  
503 as larval dispersal would be less influenced by ocean currents flowing eastwards (e.g. Southern Ocean  
504 Subtropical Front; Gersonde *et al.* 2003). In our study, demographic models showed predominant eastward  
505 migration from *J. tristani* to *J. paulensis* and from *J. lalandii* to *J. edwardsii* and a predominant westward  
506 migration from *J. frontalis* to *J. caveorum*. Although migration estimates are averaged across all events of  
507 secondary contact, these estimates reflect the predominant direction of connectivity between the *J. paulensis*  
508 – *J. tristani* and *J. edwardsii* – *J. lalandii* pairs, both influenced by the Southern Ocean Subtropical Front and  
509 the *J. frontalis* - *J. caveorum* pair, influenced by the Humboldt current (along the western coast of South  
510 America).

511         Low temperatures and sea levels during the LGM also resulted in changes in available habitat, which  
512 have possibly impacted species associated with continental shelf habitat (*J. lalandii* and *J. edwardsii*) and with  
513 seamount/islands (*J. tristani* and *J. paulensis*) differently. Schaaf (1996) used a theoretical approach  
514 to quantify the reduction/augmentation of the photic sea-bottom area (from 0 to 65 metres) during sea level  
515 fall/rise. During the LGM the global mean proportion of available habitat in the benthic photic zone was at its  
516 lowest (Fig. 4) and this shrinkage of benthic habitat was more pronounced in the continental margins than on



517 seamounts and oceanic islands (Schaaf, 1996; Fig. 5 therein). Changes in habitat area varied with the habitat  
518 and region, and were highly dependent on the amount/direction of sea level change (Schaaf 1996; Holland  
519 2012). During this period, areas in ocean ridges that were previously too deep for lobsters to inhabit might  
520 have become suitable but, at the same time, shallow areas in the continental shelf and around  
521 islands/seamounts might have become exposed and unsuitable for lobsters.

522         Transition from the LGM to the Holocene precipitated further changes in the available shallow benthic  
523 habitat for lobsters. The deglaciation of the West Antarctic Ice Sheet which was the primary source of an  
524 abrupt rise in sea level around 14,500 years ago (Clark *et al.* 2009; Fig. 4) coincided with a major expansion of  
525 available shallow benthic habitat (global averages) at around 14,000 years ago (Schaaf 1996). A southward  
526 shift in the distribution of *Jasus* spp. while tracking their thermal optima would have increased connectivity  
527 between species resulting in the recent periods of secondary contact and admixture observed in the  
528 demographic models and population genetic structure analyses, respectively. A combination of fluctuating  
529 conditions in temperature, sea level and available habitat have likely resulted in alternating periods of isolation  
530 and gene flow that have shaped the speciation processes of *Jasus* lobsters, which might still be occurring,  
531 given the recent divergence times within species pairs.

532         Our study provides genome-wide evidence of admixture between *J. paulensis* - *J. tristani*. Although  
533 George & Kensler (1970) have noted that *J. tristani* and *J. paulensis* possess a significant difference in the  
534 abdominal sculpture index, previous genetic evidence (using the mitochondrial cytochrome oxidase I gene;  
535 Groeneveld *et al.* 2012) suggests that these species can be synonymized as *J. paulensis*. Our results  
536 demonstrate that, since initial divergence, *J. tristani* and *J. paulensis* spent 4.1 times longer in secondary  
537 contact than *J. edwardsii* – *J. lalandii* and 1.2 times longer than *J. caveorum* and *J. frontalis*. The Tristan da  
538 Cunha and Gough Islands (current distribution of *J. tristani*) and the Amsterdam and St. Paul Islands (current  
539 distribution of *J. paulensis*) have been grouped in the same zoogeographic province (called the West Wind  
540 Drift Islands Province) based on endemic fish fauna distribution (Collette & Parin 1991). Archipelagic level  
541 endemism is common in marine taxa (Paulay & Meyer 2002) and has been observed for other species (e.g.

snails of the genus *Echinolittorina*; Williams & Reid 2004). Therefore, archipelagic endemism and the long periods of gene flow may explain the close relationship between *J. tristani* and *J. paulensis*.

## Conclusion

In highly dispersive marine taxa, interglacial recolonization of high-latitude habitats can occur rapidly (Hewitt 2000). Such patterns have been established for a range of Northern Hemisphere marine species (e.g. Marko 2004; Ledoux *et al.* 2018), but relatively little is known about the genetic effects of recent glaciations in the Southern Hemisphere (but see e.g. Fraser *et al.* 2009; Strugnell *et al.* 2012; Porobić *et al.* 2013). This study revealed genome-wide patterns of divergence and introgression in all extant species of a highly dispersive marine taxa for the first time. While results point to the important role of demographic and neutral processes of differentiation between species pairs, it also suggests a possible effect of selection in promoting genetic divergence between habitats. Future studies should address the role of adaptive processes to elucidate their relative contribution in shaping genome divergence and speciation of *Jasus* lobsters and to better understand how future environmental change will impact species distribution.

## Acknowledgments

Funding for this research was provided by an Australian Research Council Discovery Project grant (Project No. DP150101491) awarded to J.M.S., J.J.B., B.S.G. and N.P.M. We would like to thank Gary Carlos (University of Tasmania), Colin Fry (University of Tasmania), Daniel Ierodiaconou (Deakin University), Kent Way, Andrew Kent, Geoff Liggins, Marcus Miller, Giles Ballinger, Darrel Sykes (DAFF), Rick Webber (Te Papa Museum), Jason How (Department of Fisheries, Western Australia) and Sadie Mills (NIWA) for field assistance and sample collection; T.A.A.F. (Terres Australes et Antarctiques Françaises), for their French fisheries observer service "COPEC", the fishery observer Sophie Cascade on board the F.V. "AUSTRAL" and Charlotte Chazeau to have made available biological scientific samples and data of *Jasus paulensis* from catches in the Saint-Paul/Amsterdam French EEZ; the help of crew has also been appreciated. C.E.H was supported by FONDECYT grants #1170815 and #1201506. We would also like to thank Ira Cooke for the helpful discussions about

568 demographic modelling, the journal Editor, Alan Le Moan and two other anonymous reviewers for the  
569 constructive comments.

570

571 **Author contributions**

572 All authors contributed insights about data analysis, interpretation of results and edited the final drafts of  
573 the manuscript. C.N.S.S. analysed the data. C.N.S.S., J.M.S, B.S.G. and N.P.M. conceived the study.

574

575 **Data availability**

576 Sequencing data, pipelines for *de novo* assembly, genetic structure, environmental association and  
577 demographic inference analyses are available at:

578 [https://github.com/CatarinaNSSilva/lobsters\\_Jasus\\_demography](https://github.com/CatarinaNSSilva/lobsters_Jasus_demography).

579

580

## References

- Arendt D, King N, Carroll SB, Wittopp P, Koonin E, Kruglyak L (2016) Big Questions in Evolution. *Cell*, **166**, 528–529.
- Assis J, Tyberghein L, Bosch S, Verbruggen H, Serrão EA, De Clerck O (2018) Bio-ORACLE v2.0: Extending marine data layers for bioclimatic modelling. *Global Ecology and Biogeography*, **27**, 277–284.
- Bates D, Mächler M, Bolker BM, Walker SC (2015) Fitting linear mixed-effects models using lme4. *Journal of Statistical Software*, **67**, 1–48.
- Benardine Jeffrey I, Hale P, Degnan BM, Degnan SM (2007) Pleistocene isolation and recent gene flow in *Haliotis asinina*, an Indo-Pacific vetigastropod with limited dispersal capacity. *Molecular Ecology*, **16**, 289–304.
- Benestan L, Quinn BK, Maaroufi H, Laporte M, Clark FK, Greenwood SJ, Rochette R, Bernatchez L (2016) Seascape genomics provides evidence for thermal adaptation and current-mediated population structure in American lobster (*Homarus americanus*). *Molecular Ecology*, **25**, 5073–5092.
- Booth JD (1994) *Jasus edwardsii* Larval Recruitment off the East Coast of New Zealand. *Crustaceana*, **66**, 295–317.
- Booth JD (2006) *Jasus species*. In 'Lobsters: Biology, Management, Aquaculture and Fisheries'. (Ed. B. F. Phillips.). Blackwell Scientific Publications: Oxford.
- Booth JD, Ovenden JR (2000) Distribution of *Jasus* spp. (Decapoda: Palinuridae) phyllosomas in southern waters: Implications for larval recruitment. *Marine Ecology Progress Series*, **200**, 241–255.
- Bradford RW, Griffin D, Bruce BD (2015) Estimating the duration of the pelagic phyllosoma phase of the southern rock lobster, *Jasus edwardsii* (Hutton). *Marine and Freshwater Research*, **66**, 213–219.
- Brasher D, Ovenden J, White R (1992) Mitochondrial DNA variation and phylogenetic relationships of *Jasus* spp. (Decapoda: Palinuridae). *Journal of Zoology*, **227**, 1–16.
- Burridge CP (1999) Molecular Phylogeny of *Nemadactylus* and *Acantholatris* (Perciformes: Cirrhitidae: Cheilodactylidae), with Implications for Taxonomy and Biogeography. *Molecular Phylogenetics and Evolution*, **13**, 93–109.
- Butlin RK, Galindo J, Grahame JW (2008) Sympatric, parapatric or allopatric: The most important way to classify speciation? *Philosophical Transactions of the Royal Society B: Biological Sciences*, **363**, 2997–3007.
- Catchen J, Hohenlohe PA, Bassham S, Amores A, Cresko WA (2013) Stacks: An analysis tool set for population genomics. *Molecular Ecology*, **22**, 3124–3140.
- Catchen JM, Hohenlohe PA, Bernatchez L, Funk WC, Andrews KR, Allendorf FW (2017) Unbroken: RADseq remains a powerful tool for understanding the genetics of adaptation in natural populations. *Molecular Ecology Resources*, **17**, 362–365.
- Cayuela H, Rougemont Q, Laporte M, Mérot C, Normandeau E, Dorant Y, Tørresen OK, Hoff SNK, Jentoft S, Sirois P, Castonguay M, Jansen T, Praebel K, Clément M, Bernatchez L (2020) Shared ancestral polymorphisms and chromosomal rearrangements as potential drivers of local adaptation in a marine fish. *Molecular Ecology*, **29**, 2379–2398.
- Chiswell SM, Booth JD (1999) Rock lobster *Jasus edwardsii* larval retention by the Wairarapa Eddy off New Zealand. *Marine Ecology Progress Series*, **183**, 227–240.
- Clark PU, Dyke AS, Shakun JD, Carlson AE, Clark J, Wohlfarth B, Mitrovica JX, Hostetler SW, McCabe AM (2009) The Last Glacial Maximum. *Science*, **325**, 710–714.
- Collette BB, Parin N V (1991) Shallow-Water Fishes of Walters Shoals, Madagascar Ridge. *Bulletin of Marine Science*, **48**, 1–22.
- Crow KD, Munehara H, Bernardi G (2010) Sympatric speciation in a genus of marine reef fishes. *Molecular Ecology*, **19**, 2089–2105.
- Davis KE, Hill J, Astrop TI, Wills MA (2016) Global cooling as a driver of diversification in a major marine clade. *Nature Communications*, **7**, 1–8.
- Dodson JJ, Tremblay S, Colombani F, Carscadden JE, Lecomte F (2007) Trans-Arctic dispersals and the evolution of a circumpolar marine fish species complex, the capelin (*Mallotus villosus*). *Molecular Ecology*, **16**, 5030–5043.

Excoffier L, Dupanloup I, Huerta-Sánchez E, Sousa VC, Foll M (2013) Robust Demographic Inference from Genomic and SNP Data. *PLoS Genetics*, **9**.

Feder JL, Egan SP, Nosil P (2012) The genomics of speciation-with- gene-flow. *Trends in Genetics*, **28**, 342–350.

Fogwill CJ, Turney CSM, Hutchinson DK, Taschetto AS, England MH (2015) Obliquity Control On Southern Hemisphere Climate During The Last Glacial. *Scientific Reports*, **5**, 1–10.

Forester BR, Lasky JR, Wagner HH, Urban DL (2018) Comparing methods for detecting multilocus adaptation with multivariate genotype-environment associations. *Molecular Ecology*, 2215–2233.

Fraser CI, Nikula R, Spencer HG, Waters JM (2009) Kelp genes reveal effects of subantarctic sea ice during the Last Glacial Maximum. *Proceedings of the National Academy of Sciences of the United States of America*, **106**, 3249–3253.

George RW, Kensler CB (1970) Recognition of marine spiny lobsters of the *Jasus lalandii* group (crustacea: Decapoda: Palinuridae). *New Zealand Journal of Marine and Freshwater Research*, **4**, 292–311.

Gersonde R, Abelman A, Brathauer U, Becquey S, Bianchi C, Cortese G, Grobe H, Kuhn G, Niebler HS, Segl M, Sieger R, Zielinski U, Fütterer DK (2003) Last glacial sea surface temperatures and sea-ice extent in the Southern Ocean (Atlantic-Indian sector): A multiproxy approach. *Paleoceanography*, **18**.

Gosselin T (2017) radiator: RADseq Data Exploration, Manipulation and Visualization using R. R package version 0.0.5.

Goudet J (2005) HIERFSTAT, a package for r to compute and test hierarchical F-statistics. *Molecular Ecology Notes*, **5**, 184–186.

Groeneveld JC, von der Heyden S, Matthee CA (2012) High connectivity and lack of mtDNA differentiation among two previously recognized spiny lobster species in the southern Atlantic and Indian Oceans. *Marine Biology Research*, **8**, 764–770.

Gutenkunst RN, Hernandez RD, Williamson SH, Bustamante CD (2009) Inferring the joint demographic history of multiple populations from multidimensional SNP frequency data. *PLoS Genetics*, **5**.

Hewitt G (2000) The genetic legacy of the Quaternary ice ages. *Nature*, **405**, 907–913.

Hinojosa I, Gardner C, Green B, Jeffs A (2018) Coastal chemical cues for settlement of the southern rock lobster, *Jasus edwardsii*. *Bulletin of Marine Science*, 1–16.

Hinojosa IA, Green BS, Gardner C, Hesse J, Stanley JA, Jeffs AG (2016) Reef sound as an orientation cue for shoreward migration by pueruli of the rock lobster, *Jasus edwardsii*. *PLoS ONE*, **11**, 1–15.

Holland SM (2012) Sea level change and the area of shallow-marine habitat: implications for marine biodiversity. *Paleobiology*, **38**, 205–217.

Holthuis LB (1991) *Marine lobsters of the world. An annotated and illustrated catalogue of species of interest to fisheries known to date. FAO Fisheries Synopsis. No. 125, Vol. 13. Rome, FAO.*

Holthuis LB, Sivertsen E (1967) *The Crustacea Decapoda, Mysidacea and Cirripedia of the Tristan da Cunha Archipelago, with a revision of the “frontalis” subgroup of the genus Jasus. Res. Norv. Scient. Exp. Tristan da Cunha 1937-1938*, **52**, 1-55.

Huybrechts P (2002) Sea-level changes at the LGM from ice-dynamic reconstructions of the Greenland and Antarctic ice sheets during the glacial cycles. *Quaternary Science Reviews*, **21**, 203–231.

Jenkins TL, Ellis CD, Triantafyllidis A, Stevens JR (2019) Single nucleotide polymorphisms reveal a genetic cline across the northeast Atlantic and enable powerful population assignment in the European lobster. *Evolutionary Applications*, 1–19.

Jombart T (2008) Adegnet: A R package for the multivariate analysis of genetic markers. *Bioinformatics*, **24**, 1403–1405.

Kenchington EL, Harding GC, Jones MW, Prodöhl P a (2009) Pleistocene glaciation events shape genetic structure across the range of the American lobster, *Homarus americanus*. *Molecular Ecology*, **18**, 1654–67.

Kilian A, Wenzl P, Huttner E, Carling J, Xia L, Blois H, Caig V, Heller-Uszynska K, Jaccoud D, Hopper C, Aschenbrenner-Kilian M, Evers M, Peng K, Cayla C, Hok P, Uszynski G (2012) Diversity Arrays Technology: A Generic Genome Profiling Technology on Open Platforms. In: *Data Production and Analysis in Population Genomics. Methods in Molecular Biology, vol 888.* (eds Pompanon F, Bonin A),

pp. 67–89. Humana Press, Totowa.

Ledoux JB, Frleta-Valić M, Kipson S, Antunes A, Cebrian E, Linares C, Sánchez P, Leblois R, Garrabou J (2018) Postglacial range expansion shaped the spatial genetic structure in a marine habitat-forming species: Implications for conservation plans in the Eastern Adriatic Sea. *Journal of Biogeography*, **45**, 2645–2657.

Linck E, Battey CJ (2019) Minor allele frequency thresholds strongly affect population structure inference with genomic data sets. *Molecular Ecology Resources*, **19**, 639–647.

Lowe WH, Allendorf FW (2010) What can genetics tell us about population connectivity? *Molecular ecology*, **19**, 3038–51.

Manel S, Holderegger R (2013) Ten years of landscape genetics. *Trends in Ecology and Evolution*, **28**, 614–621.

Marko PB (2004) “What’s larvae got to do with it?” Disparate patterns of post-glacial population structure in two benthic marine gastropods with identical dispersal potential. *Molecular Ecology*, **13**, 597–611.

Matthee CA, Cockcroft AC, Gopal K, von der Heyden S (2007) Mitochondrial DNA variation of the west-coast rock lobster, *Jasus lalandii*: Marked genetic diversity differences among sampling sites. *Marine and Freshwater Research*, **58**, 1130–1135.

Meirmans PG, Van Tienderen PH (2004) Genotype and Genodive: Two Programs for the Analysis of Genetic Diversity of Asexual Organisms. *Molecular Ecology Notes*, **4**, 792–794.

Le Moan A, Gagnaire PA, Bonhomme F (2016) Parallel genetic divergence among coastal-marine ecotype pairs of European anchovy explained by differential introgression after secondary contact. *Molecular Ecology*, **25**, 3187–3202.

Momigliano P, Jokinen H, Fraimout A, Florin A-B, Norkko A, Merilä J (2017) Extraordinarily rapid speciation in a marine fish. *Proceedings of the National Academy of Sciences*, **114**, 6074–6079.

Obbard DJ, MacLennan J, Kim KW, Rambaut A, O’Grady PM, Jiggins FM (2012) Estimating divergence dates and substitution rates in the drosophila phylogeny. *Molecular Biology and Evolution*, **29**, 3459–3473.

Oksanen J, Blanchet F, Friendly M, Kindt R, Legendre P, McGlinn D, Minchin PR, O’Hara RB, Simpson GL, Solymos P, Stevens MHH, Szoecs E, Wagner H (2019) vegan: Community Ecology Package. R package version 2.5-6.

Olivieri I, Tonnabel J, Ronce O, Mignot A (2016) Why evolution matters for species conservation: Perspectives from three case studies of plant metapopulations. *Evolutionary Applications*, **9**, 196–211.

Ovenden JR (2013) Crinkles in connectivity: combining genetics and other types of biological data to estimate movement and interbreeding between populations. *Marine and Freshwater Research*, **64**, 201.

Ovenden JR, Booth JD, Smolenski AJ (1997) Mitochondrial DNA phylogeny of red and green rock lobsters (genus *Jasus*). *Marine and Freshwater Research*, **48**, 1131–1136.

Ovenden JR, Brasher DJ, White RWG (1992) Mitochondrial DNA analyses of the red rock lobster *Jasus edwardsii* supports an apparent absence of population subdivision throughout Australasia. *Marine Biology*, **112**, 319–326.

Palero F, Lopes J, Abelló P, Macpherson E, Pascual M, Beaumont MA (2009) Rapid radiation in spiny lobsters (*Palinurus* spp) as revealed by classic and ABC methods using mtDNA and microsatellite data. *BMC Evolutionary Biology*, **9**, 263.

Paris JR, Stevens JR, Catchen JM (2017) Lost in parameter space: a road map for stacks. *Methods in Ecology and Evolution*, **8**, 1360–1373.

Paulay G, Meyer C (2002) Diversification in the tropical Pacific: Comparisons between marine and terrestrial systems and the importance of founder speciation. *Integrative and Comparative Biology*, **42**, 922–934.

Pecl G, Frusher S, Gardner C, Haward M, Hobday A, Jennings S, Nursey-Bray M, Punt A, Revill H, van Putten I (2009) *The east coast Tasmanian rock lobster fishery – vulnerability to climate change impacts and adaptation response options. Report to the Department of Climate Change, Australia.*

Phillips BF (2013) *Lobsters: Biology, Management, Aquaculture and Fisheries* (BF Phillips, Ed.). Department of Environment & Agriculture, Curtin University, Western Australia.

Pickrell JK, Pritchard JK (2012) Inference of Population Splits and Mixtures from Genome-Wide Allele

Frequency Data. *PLoS Genetics*, **8**, e1002967.

Pinheiro HT, Bernardi G, Thorrold, Simon R, Joyeux J-C, Macieira RM, Gasparini JL, Rocha C, Rocha LA (2017) Island biogeography of marine organisms. *Nature*, **549**, 82–85.

Pollock DE (1990) Palaeoceanography and Speciation in the Spiny Lobster Genus *Jasus*. *Bulletin of Marine Science*, **46**, 387–405.

Porobić J, Canales-Aguirre CB, Ernst B, Galleguillos R, Hernández CE (2013) Biogeography and historical demography of the Juan Fernández rock lobster, *Jasus frontalis* (Milne Edwards, 1837). *Journal of Heredity*, **104**, 223–233.

Reich D, Thangaraj K, Patterson N, Price AL, Singh L (2009) Reconstructing Indian population history. *Nature*, **461**, 489–494.

Rocha LA, Robertson DR, Roman J, Bowen BW (2005) Ecological speciation in tropical reef fishes. *Proceedings of the Royal Society B: Biological Sciences*, **272**, 573–579.

Rochette NC, Catchen JM (2017) Deriving genotypes from RAD-seq short-read data using Stacks. *Nature Protocols*, **12**, 2640–2659.

Rougemont Q, Bernatchez L (2018) The demographic history of Atlantic salmon (*Salmo salar*) across its distribution range reconstructed from approximate Bayesian computations\*. *Evolution*, **72**, 1261–1277.

Rougeux C, Bernatchez L, Gagnaire PA (2017) Modeling the multiple facets of speciation-with-gene-flow toward inferring the divergence history of lake whitefish species pairs (*Coregonus clupeaformis*). *Genome Biology and Evolution*, **9**, 2057–2074.

Sakamoto Y, Ishiguro M, Kitagawa G (1986) *Akaike Information Criterion Statistics*. D. Reidel.

Sandoval-Castillo J, Robinson NA, Hart AM, Strain LWS, Beheregaray LB (2018) Seascape genomics reveals adaptive divergence in a connected and commercially important mollusc, the greenlip abalone (*Haliotis laevigata*), along a longitudinal environmental gradient. *Molecular Ecology*, **27**, 1603–1620.

Schaaf A (1996) Sea level changes, continental shelf morphology, and global paleoecological constraints in the shallow benthic realm: a theoretical approach. *Palaeogeography, Palaeoclimatology, Palaeoecology*, **121**, 259–271.

Silva CNS, Villacorta-Rath C, Woodings LN, Murphy NP, Green BS, Hartmann K, Gardner C, Bell JJ, Strugnelli JM (2019) Advancing our understanding of the connectivity, evolution and management of marine lobsters through genetics. *Reviews in Fish Biology and Fisheries*, **29**, 669–687.

Smadja CM, Butlin RK (2011) A framework for comparing processes of speciation in the presence of gene flow. *Molecular Ecology*, **20**, 5123–5140.

Sorenson L, Allen GR, Erdmann M V., Dai CF, Liu SYV (2014) Pleistocene diversification of the *Pomacentrus coelestis* species complex (Pisces: Pomacentridae): historical biogeography and species boundaries. *Marine Biology*, **161**, 2495–2507.

Souissi A, Bonhomme F, Machado M, Bahri-Sfar L, Gagnaire P-A (2018) Genomic and geographic footprints of differential introgression between two divergent fish species (*Solea* spp.). *Heredity*, **121**, 579–593.

Stanley JA, Hesse J, Hinojosa IA, Jeffs AG (2015) Inducers of settlement and moulting in post-larval spiny lobster. *Oecologia*, **178**, 685–697.

Strugnelli JM, Watts PC, Smith PJ, Allcock AL (2012) Persistent genetic signatures of historic climatic events in an Antarctic octopus. *Molecular Ecology*, **21**, 2775–2787.

Thomas L, Bell JJ (2013) Testing the consistency of connectivity patterns for a widely dispersing marine species. *Heredity*, **111**, 345–54.

Tine M, Kuhl H, Gagnaire P, Louro B, Desmarais E, Martins RST, Hecht J, Knaust F, Belkhir K, Klages S, Dieterich R, Stueber K, Piferrer F, Guinand B, Bierne N, Volckaert FAM, Bargelloni L, Power DM, Bonhomme F *et al.* (2014) European sea bass genome and its variation provide insights into adaptation to euryhalinity and speciation. *Nature Communications*, **5**, 5770.

Titus BM, Blischak PD, Daly M (2019) Genomic signatures of sympatric speciation with historical and contemporary gene flow in a tropical anthozoan (Hexacorallia: Actiniaria). *Molecular Ecology*, 3572–3586.

Villacorta-Rath C, Ilyushkina I, Strugnelli JM, Green BS, Murphy NP, Doyle SR, Hall NE, Robinson AJ, Bell JJ (2016) Outlier SNPs enable food traceability of the southern rock lobster, *Jasus edwardsii*. *Marine*

785 *Biology*, **163**, 1–11.

786 Villacorta-Rath C, Souza CA, Murphy NP, Green BS, Gardner C, Strugnelli JM (2018) Temporal genetic patterns  
787 of diversity and structure evidence chaotic genetic patchiness in a spiny lobster. *Molecular Ecology*, **27**,  
788 54–65.

789 Webber WR, Booth JD (1995) A new species of *Jasus* (Crustacea: Decapoda: Palinuridae) from the eastern  
790 South Pacific Ocean. *New Zealand Journal of Marine and Freshwater Research*, **29**, 613–622.

791 Weigelt P, Steinbauer MJ, Cabral JS, Kreft H (2016) Late Quaternary climate change shapes island  
792 biodiversity. *Nature*, **532**, 99–102.

793 Williams ST, Reid DG (2004) Speciation and diversity on tropical rocky shores: A global phylogeny of snails of  
794 the genus *Echinolittorina*. *Evolution*, **58**, 2227–2251.

795

796